Towards Congestion Management in Distribution Networks

DOI:
10.1049/icp.2023.0128

Document status and date:
Published: 29/05/2023

Document Version:
Accepted manuscript including changes made at the peer-review stage

Towards Congestion Management in Distribution Networks: a Dutch Case Study on Increasing Heat Pump Hosting Capacity

Sen Zhan*, Tongyou Gu†, Wouter van den Akker*‡, Willemijn Brus†, Anne van der Molen*§, Johan Morren*¶
*Department of Electrical Engineering, Eindhoven University of Technology, Eindhoven, The Netherlands
†Qirion Energy Consulting, Alliander, Arnhem, The Netherlands
‡Innovation Department, Alliander, Arnhem, The Netherlands
§Grid Strategy Department, Stedin, Rotterdam, The Netherlands
¶Department of Asset Management, Enexis, 's-Hertogenbosch, The Netherlands
Emails: {s.zhan, w.f.v.d.akker, a.e.v.d.molen, j.morren}@tue.nl, {tongyou.gu, willemijn.brus}@qirion.nl

Abstract—**The current high gas prices motivate end-users to replace their gas heating with electric heat pumps. This will likely cause frequent congestion issues in low-voltage (LV) distribution grids and slow down the heat pump adoption rate. To avoid or defer the expensive and complicated grid expansion, this study shares a solution approach of a Dutch Distribution System Operator (DSO) to enable the increasing adoption of heat pumps in existing dense housing areas. Data of the DSO and a local housing company have been combined to investigate the heat pump hosting capacity on a dense urban LV feeder, including realistic data of grid topology, load and heat dynamics, and practical operating characteristics of heat pumps. Our simulation compares two control strategies: (1) individual peak shaving and (2) central optimal power flow control. We show the central optimal power flow control with end-users' thermal comfort constraints and an objective function of minimizing losses can smoothen total grid loading and lead to flat voltage profiles. This allows the approach to be robust against baseload forecast errors, while the individual peak shaving is more prone to such errors. Moreover, by simulating the strategies on the worst-case scenarios where heat pumps are allocated to end-users at the end of the feeder, we determine the individual peak shaving strategy can slightly increase the heat pump hosting capacity from 49% where no control is imposed to 51%, while the central optimal power flow control allows 100% heat pump connections without causing grid congestion. Finally, recommendations to increase the heat pump hosting capacity are given based on simulation results.**

Index Terms—**Congestion management, optimal power flow control, peak shaving, hosting capacity, heat pump, LV grid**

I. Introduction

The current high gas price peaks and severe concern of gas shortages in Europe motivate residential end-users to replace their gas heating with electric heat pumps. This brings new security of supply issues to LV electrical networks as those networks were designed decades ago without foreseeing these heavy loads. Network congestion is observed characterized by overloading of transformers and cables, and voltage limit violations, which limit the pace of the heating electrification. The traditional solution to those congestion issues is expanding existing grids. This requires significant investments, but more problematic is the long time to implement the expansion in the crowded underground of urbanized areas. Alternative smart grid solutions are therefore seen as essential to keep pace in the energy transition and support the continuously occurring household electrification, which typically involve exploring the flexibility of grid assets and household appliances.

Tremendous research efforts have been made to alleviate congestion problems for distribution networks, which can be categorized into market-based strategies [1]–[3], dynamic pricing schemes, e.g. distribution locational marginal pricing (DLMP) [4], [5], transactive energy (TE) [6], [7], and technical control approaches. Despite that appealing simulation results were reported in the literature for market-based or dynamic pricing-based strategies, several challenges have to be confronted for their practical implementation, such as lack of liquidity, manipulation, settlement, baselining [8], price inelasticity, and introduction of new power peaks. Under technical control approaches, DSOs or aggregators dispatch controllable assets by often solving an optimal power flow control problem considering grid limits, either through explicit network modelling [9]–[11] or utilizing voltage sensitivity information [12], [13]. Regulation and privacy concerns with DSOs controlling household appliances can be potentially addressed by negotiating flexibility usage contracts with end-users incorporating end-users' comfort settings and introducing tariff benefits. Finally, an extensive assessment framework for various congestion management mechanisms was introduced in [14].

To accelerate the DSOs' adoption of these relatively simple and effective technical control approaches, this paper shares a solution approach of a Dutch DSO in a city housing area with an existing LV feeder. Approximately 70% of the houses are being renovated by the housing company by replacing gas heating with heat pumps. The main contributions of this study are:

- A real Dutch case study on increasing the heat pump hosting capacity for a local housing company is conducted, which includes realistic data of topology, load, and heat dynamics, and practical heat pump operating constraints.
- An individual peak shaving and a central power flow control are simulated with focuses on grid congestion alleviation and end-users' thermal comfort preservation.
- Recommendations are given to increase the heat pump hosting capacity based on the simulation results.

The remainder of this paper is organized as follows. Section II describes the component models. Section III presents the individual peak shaving strategy and the central optimal power flow control. Section IV reports a case study and simulation results. Conclusions are drawn in Section V.

II. System models

This section presents models for the household heating and distribution networks. Notations are provided in Table I. An overview of the household heating system is available in [15]. For simplicity, we neglect the buffer tank for space heating as it is very small in our case (around 20 liters) which is not comparable to the building concerning thermal capacitance.

This work is funded by TKI Energie from the 'Toeslag voor Topconsortia voor Kennis en Innovatie (TKI)' under reference 1821401.

A. Heat Pump Model

$$u_1 = 0, u_t \in \{0,1\}, \forall t = 2, \cdots, T+1 \tag{1a}$$
$$u_{t+1} - u_t - u_\tau \leq 0, \forall \tau = t+2, \cdots, t+\underline{T}^{on}, \quad \forall t = 1, \cdots, T-1 \tag{1b}$$
$$u_t - u_{t+1} + u_\tau \leq 1, \forall \tau = t+2, \cdots, t+\underline{T}^{off}, \quad \forall t = 1, \cdots, T-1 \tag{1c}$$
$$u_t = u_t^{sh} + u_t^{dhw}, \forall t = 1, \cdots, T+1 \tag{1d}$$
$$p_t^{sh} = u_{t+1}^{sh} P^{hp}, p_t^{dhw} = u_{t+1}^{dhw} P^{hp}, \forall t = 1, \cdots, T \tag{1e}$$

The heat pump system is modeled as (1). The node index is dropped for clarity. As shown in (1a), the heat pump operation is a discrete decision, which can be either turned-on or turned-off assuming no other continuous control possibility. The starting state of the heat pump is set as turned-off. The inequality constraint (1b) is imposed to reflect the minimum online time of the heat pump. Specifically, the first two terms in (1b) are evaluated to be 1 if and only if the heat pump is switched on at time $t+1$. Then the heat pump has to stay online for the subsequent time steps τs to satisfy (1b). Likewise, the minimum offline time is imposed in (1c). These constraints (1b)-(1c) avoid too frequent operation of the heat pump based on practical heat pump lifetime considerations. Finally, the constraints (1d) and (1e) impose that the heat pump can either be used for space heating or domestic hot water at one time step.

B. Space Heating Model

$$T_1^{ind} = T_{set}^{ind} \tag{2a}$$
$$C^{sh}(T_{t+1}^{ind} - T_t^{ind}) = \Delta t[p_t^{sh}\text{CoP}_t^{sh} - \frac{1}{R^{sh}}(T_t^{ind} - T_t^{out})], \forall t \in 1, \cdots, T \tag{2b}$$
$$T_{min}^{ind} \leq T_{t+1}^{ind} \leq T_{max}^{ind}, \forall t \in 1, \cdots, T \tag{2c}$$

The space heating is modeled in (2) using a resistance-capacitance (RC) model [16], in which (2a) sets the initial temperature. A discrete heat dynamics model is shown in (2b), where the temperature change is associated with heat pump supply and thermal loss. The last constraint (2c) includes the thermal comfort settings of end-users.

C. Domestic Hot Water Model

$$T_1^{dhw} = T_{set}^{dhw} \tag{3a}$$
$$c^{water} m^{tank}(T_{t+1}^{dhw} - T_t^{dhw}) = \Delta t[p_t^{dhw}\text{CoP}_t^{dhw} - c^{water}\dot{m}_t^{dhw}(T_t^{dhw} - T^{inlet})], \forall t \in 1, \cdots, T \tag{3b}$$
$$T_{min}^{dhw} \leq T_{t+1}^{dhw} \leq T_{max}^{dhw}, \forall t \in 1, \cdots, T \tag{3c}$$

Likewise, the domestic hot water model is presented in (3). The constraints (3a) and (3c) are similar to that above, imposing respectively initial temperature and temperature limits for the thermal comfort of end-users. A hot water heat dynamics model is in (3b), where the hot water temperature is affected by heat pump supply and the flow rate of inlet cold water, which is assumed the same as the rate of hot water supply.

D. Distribution Network Model

To study the impacts of heat pump loads on the distribution grid, the linearized branch flow model [17] is adopted to characterize bus voltage and cable loading which is built upon the assumption that branch losses are negligible. The model is formulated as (4). The time index is dropped by clarity. The active and reactive power balance is imposed in (4a) and (4b) respectively. We consider baseload and heat pump loads, while other heavy loads such as electric vehicles are not included as the studied case is for a social housing company[1]. The constraint (4c) dictates the nodal voltage relation across cables. Finally, grid limits are enforced in (4d)-(4e), on thermal limits of cables and statutory voltage limits respectively.

TABLE I
NOTATION FOR OPTIMIZATION MODEL.

Notation	Physical meaning	Unit
$\mathcal{N}, \mathcal{E}, \mathcal{H}$	Sets of nodes, cables, and households	-
$T, \Delta t$	Time horizon length, time step length	hour
Parameters		
$\underline{T}^{on}, \overline{T}^{off}$	Minimum online/offline time length	hour
P^{hp}	Heat pump capacity	kW
T_{set}^{ind}	Target indoor temperature	°C
T_{set}^{dhw}	Target hot water temperature	°C
C^{sh}	Thermal capacitance for space heating	kWh/K
R^{sh}	Thermal resistance for space heating	$(\text{kW/K})^{-1}$
CoP_t^{sh}	CoP of heat pump for space heating at time t	-
CoP_t^{dhw}	CoP of heat pump for hot water at time t	-
T_t^{out}	Outdoor temperature at time t	°C
T^{inlet}	Inlet cold water temperature	°C
$T_{min}^{ind}, T_{max}^{ind}$	Minimum/maximum indoor temperature	°C
$T_{min}^{dhw}, T_{max}^{dhw}$	Minimum/maximum hot water temperature	°C
c^{water}	Thermal capacitance of water	kWh/kg/K
m^{tank}	Water mass in hot water tank	kg
$\dot{m}_t^{dhw}$	Hot water flow rate	kg/hour
p_j^{base}, q_j^{base}	Active and reactive baseload at node j	kW/kVar
$\tan\phi^{hp}$	Reactive to active power ratio of heat pump	
r_{ij}, x_{ij}	Cable resistance/reactance between node i and j	$k\Omega$
v_j^{min}, v_j^{max}	Min/max voltage magnitude squared of node j	$(\text{kV})^2$
v^{ref}	Reference voltage magnitude squared	$(\text{kV})^2$
S_{ij}^{max}	Max cable apparent power between node i and j	kVA
$\overline{p}^{base}$	Baseload threshold for peak shaving strategy	kW
Variables		
u_t	Online/offline state of heat pump at time t	-
u_t^{sh}, u_t^{dhw}	Online/offline state of heat pump for space heating and domestic hot water use at time t	-
p_t^{sh}, p_t^{dhw}	Heat pump power output for space heating and domestic hot water use at time t	kW
T_t^{ind}	Indoor temperature at time t	°C
T_t^{dhw}	Hot water temperature at time t	°C
$p_{j,t}^{hp}$	Heat pump power output at node j time t	kW
Dependent		
P_{ij}, Q_{ij}	Active/reactive power flow from node i to j	kW
v_j	Voltage magnitude squared of node j	$(\text{kV})^2$

$$\sum_{i:i\to j} P_{ij} = \sum_{k:j\to k} P_{jk} + p_j^{base} + p_j^{hp}, \forall j \in \mathcal{N} \tag{4a}$$
$$\sum_{i:i\to j} Q_{ij} = \sum_{k:j\to k} Q_{jk} + q_j^{base} + \tan\phi^{hp} p_j^{hp}, \forall j \in \mathcal{N} \tag{4b}$$
$$v_j = v_i - 2\left(r_{ij}P_{ij} + x_{ij}Q_{ij}\right), \forall (i,j) \in \mathcal{E} \tag{4c}$$
$$P_{ij}^2 + Q_{ij}^2 \leq (S_{ij}^{max})^2, \forall (i,j) \in \mathcal{E} \tag{4d}$$
$$v_j^{min} \leq v_j \leq v_j^{max}, \forall j \in \mathcal{N} \tag{4e}$$

[1]Different from private housing, social housing in the Netherlands is intended for people with lower incomes.

III. Control Models

In this study, we develop an individual peak shaving strategy and a central optimal power flow control strategy for heat pump management. As the benchmark, an unmanaged heat pump use is also simulated. Details are presented below.

A. Unmanaged Heat Pump Use

In the unmanaged heat pump use case, the heat pumps are operated to track the target temperature for space heating and domestic hot water as closely as possible based on end-users' instant heat demand. As shown in (5), the optimization problem minimizes deviations to the target temperature for space heating and hot water taking the heat pump model, space heating model, and domestic hot water model as constraints.

$$\min_{p_t^{hp}} \sum_{t=1,\cdots,T+1} |T_t^{ind} - T_{set}^{ind}| + |T_t^{dhw} - T_{set}^{dhw}| \tag{5a}$$

$$\text{s.t. } (1), (2), (3) \tag{5b}$$

B. Individual Peak Shaving

Likewise, the individual peak shaving strategy adopts a similar formulation except introducing an additional penalty term in the objective function where M is an arbitrarily large parameter, which motivates the heat pump to be turned off when the baseload forecast is higher than a given pre-defined threshold $\overline{p}^{base}$. This is likely to reduce the peak power consumption from the households and thus alleviate network congestion. It is worth noting that there is no coordination between households under this individual peak shaving strategy. The DSO determines this threshold by analyzing smart meter baseload data, balancing between the effectiveness of this strategy which requires a lower threshold and the thermal comfort of end-users which leans towards a higher threshold.

$$\min_{p_t^{hp}} \sum_{t=1,\cdots,T+1} |T_t^{ind} - T_{set}^{ind}| + |T_t^{dhw} - T_{set}^{dhw}| + \sum_{t \text{ such that } p_t^{base} \geq \overline{p}^{base} \text{ for } t=1,\cdots,T} M u_{t+1} \tag{6a}$$

$$\text{s.t. } (1), (2), (3) \tag{6b}$$

C. Central Optimal Power Flow Control

The central optimal power flow control is based on a different design, which explores the coordination between households. Under this strategy, the DSO centrally collects required parameters in the model (7) and dispatches heat pumps based on the optimal solutions. Although the DSO takes a more intrusive role in this design, the strategy is more likely to optimally use grid capacity and resolve network congestion while considering the thermal comfort settings of end-users, avoiding the risk of severe consequences such as blackouts and drastic loss of thermal comfort. The formulation in (7) employs an objective function minimizing power losses, which not only increases the accuracy of the linearized branch flow model but also smoothens grid loading throughout the simulation horizon. As an illustrative case, suppose in total two units of power have to be delivered to a household at two consecutive time steps. The even allocation of one unit per time step will result in the smallest loss compared to other allocation plans due to the quadratic accumulation of losses. By minimizing losses, the optimization model (7) will likely return a grid loading that is smooth throughout the horizon. Finally, the additional constraints (7c) ensure that the thermal comfort of end-users for the next simulation horizon is not impacted.

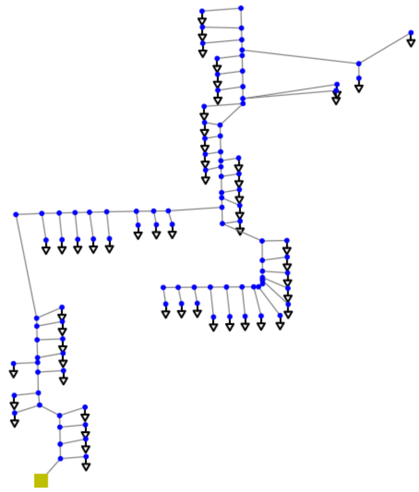

Fig. 1. Network topology including 53 residential households, of which 37 are from the local housing company and are intended to replace their gas heating with electric heat pumps.

$$\min_{p_{j,t}^{hp}} \sum_{t=1,\cdots,T} \sum_{(i,j)\in\mathcal{E}} \frac{(P_{ij,t})^2 + (Q_{ij,t})^2}{v^{ref}} r_{ij} \tag{7a}$$

$$\text{s.t. } (1), (2), (3), (4) \tag{7b}$$

$$T_{j,T+1}^{dhw} \geq T_{set}^{dhw}, T_{j,T+1}^{ind} \geq T_{set}^{ind}, \forall j \in \mathcal{H} \tag{7c}$$

IV. Case Study

A. Case Description

The studied LV feeder presented in Fig. 1 includes 53 residential end-users, of which 37 are from the housing company. As shown in Fig. 2, anonymous smart meter readings from a local DSO with a resolution of 15 minutes are used to represent the baseload. Two severe winter days' profiles are extracted wherein the first day's profiles are assumed as the baseload forecast for the second day. The tool in [18] can also be used to generate synthetic profiles. The heat pumps are assumed to have a capacity of 2.89 kW and a power factor of 0.99, with the minimum online and offline time of both 45 minutes. The coefficient of performance (CoP) for air-source heat pumps under different temperature conditions is taken from [19].

The simulation is performed on a cold winter day with an average outdoor temperature of -8.4°C, shown in Fig. 3. The target indoor temperature is 20°C, with a minimum of 19°C and a maximum of 21°C for the thermal comfort of end-users. The heat transfer coefficient which equals $1/R^{sh}$ for the households is determined as 0.225 kW/K by an external consulting company. The thermal capacitance is taken from [16] as 20 kWh/K. Comparing the heat transfer coefficient with others reported in [16], it is obvious that the households from the housing company are not well-insulated, which require more energy to keep the needed indoor temperature. For domestic hot water use, the water tank is 200 liters. The target temperature is 55°C, with a minimum of 45°C and a maximum of 100°C. The inlet cold tap water temperature is 10°C as in [15]. The hot water flow rate profiles are generated from the tool developed in [20], assuming four categories, an average daily use of 120 liters, and a maximum flow rate of 300 liters per hour, which are visualized in Fig. 4.

The voltage limits are set as 0.96 per unit and 1.04 per unit for the minimum and the maximum values respectively to safely stay within the 10% margin considering the impacts from upstream medium-voltage grids. The baseload threshold for the

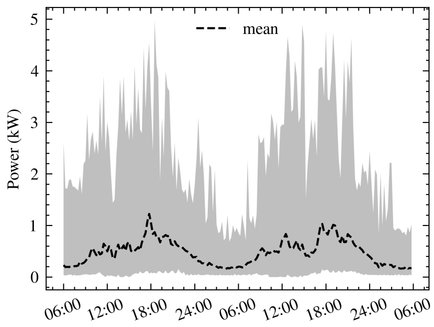

Fig. 2. Base load profiles.

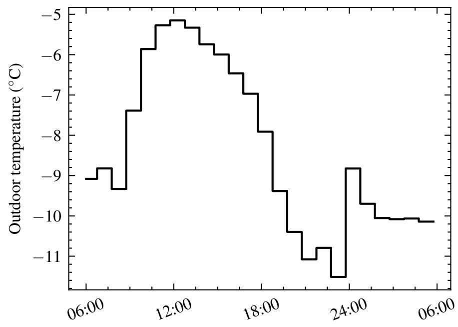

Fig. 3. Outdoor temperature.

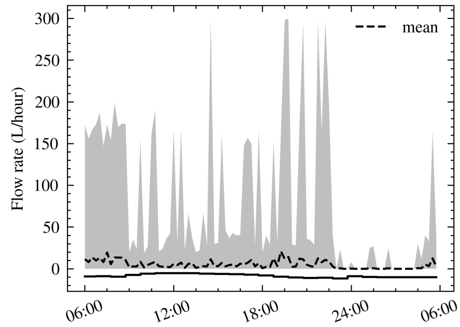

Fig. 4. Hot water flow rates.

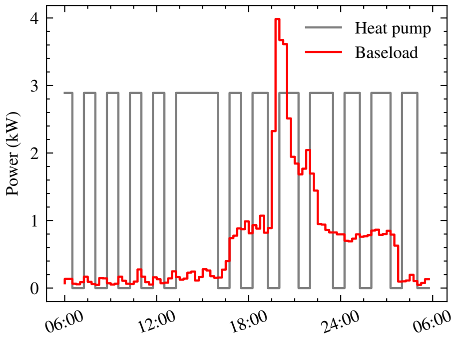

Fig. 5. Example HP profile with base case.

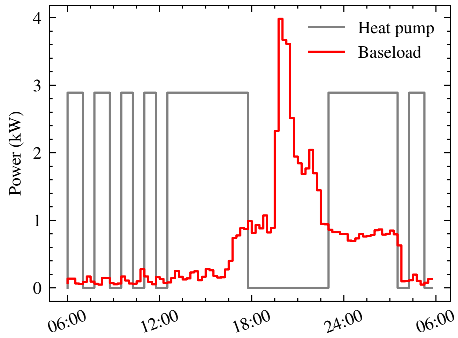

Fig. 6. Example HP profile with peak shaving.

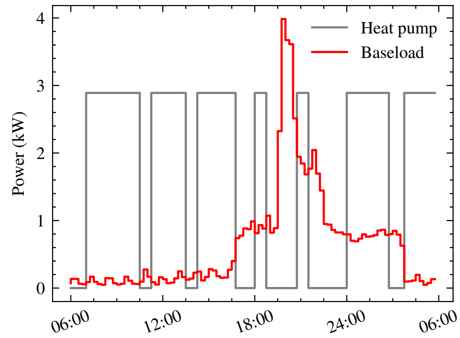

Fig. 7. Example HP profile with power flow control.

individual peak shaving strategy is determined by the local DSO as 0.9 kW. The optimization problems are solved with the solver Gurobi. The individual optimization problems are carried out with a time limit of 120 seconds and an optimality gap setting of 0.1%. The central optimization is executed with a time limit of 7200 seconds and the same optimality gap. The optimized heat pump profiles with baseload profiles are fed to a non-linear power flow solver to extract grid states.

B. Results

1) Heat Pump Profiles: To show the effectiveness of the two control strategies, Figs. 5 to 7 visualize the heat pump profiles at the base case, the peak shaving case, and the central optimal power flow control case for a household respectively. Comparing Fig. 6 to Fig. 5, it is clear that the heat pump is forced to be turned off during high baseload, avoiding the coincidence of the peak baseload and heat pump load. To maintain thermal comfort for the end-users, the heat pump stays on before the evening to create a thermal buffer for the household. Although not explicitly modelled as in the individual peak shaving case, the central optimal power flow control strategy also avoids heat pump consumption when the baseload is at the highest level. Different from the peak shaving strategy, it starts to heat the household early in the morning when the baseload is negligible. This allows the end-users to make better use of the grid capacity.

2) Impacts on Distribution Grid: The impacts of unmanaged and managed heat pump loads on the distribution grid are presented in Figs. 8 to 13. Specifically, Figs. 8 to 10 show the bus voltage and cable loading analyzed using the unmanaged and managed heat pump profiles and baseload data from the first day, which are also used as baseload forecast in the respective models. It is clear that the peak shaving strategy can alleviate network congestion, while the central optimal power flow control can maintain smooth voltage and loading profiles throughout the simulation horizon. This allows the model to work with forecast errors. As seen in Figs. 11 to 13, when the managed heat pump profiles are tested with baseload of the second day, the central optimal power flow control is still able to fully resolve network congestion, while severe congestion issues are observed for the individual peak shaving. The total load for the test feeder is shown in Figs. 14 to 16 for different cases. It is clear in the central power flow control case the heat pump load is mostly allocated to hours when the baseload is low, leading to a flat loading at the beginning of the feeder, reducing the maximum load by 22% and 17% compared to the base case and peak shaving respectively.

3) Impacts on Thermal Comfort: The indoor temperature and the hot water temperature which are the key parameters to assess the thermal comfort of end-users are presented in Figs. 17 to 19. The unmanaged heat pump operation maintains the most stable temperature profiles, leading to the best thermal comfort. The individual peak shaving and the central optimal power flow control can however exploit the flexibility of the household heating for distribution grid management while complying with the temperature settings of end-users.

4) Hosting Capacity and Impacts of House Insulation: Finally, we evaluate the heat pump hosting capacity for the test feeder, which is determined as the maximum percentage of heat pump connections for the households from the local housing company without causing network congestion. We work with the worst-case arrangement where heat pumps are allocated to end-users located at the end of the feeder. Figs. 20 and 21 show the minimum voltage and the maximum loading with an increasing amount of heat pump connections for the accurate forecast and working forecast cases respectively. Note in the latter case the first day's baseload is taken as the forecast for the next day. It is determined that the hosting capacity is 49% for the unmanaged case and 100% for the central optimal power flow control with both forecast accuracies. For the peak shaving, with an accurate baseload forecast, the hosting capacity is 76%. While with a working forecast algorithm, the hosting capacity is 51%. This highlights the importance of an accurate baseload forecast for the peak shaving strategy. Finally, we study the impact of better insulation for the households. We determine from Fig. 22 that

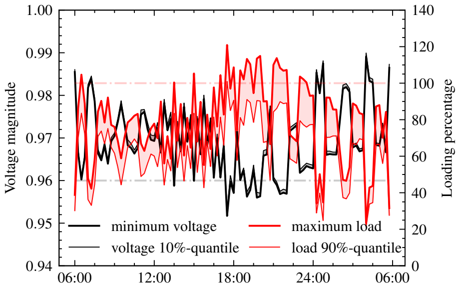

Fig. 8. Grid states at base case at day 1.

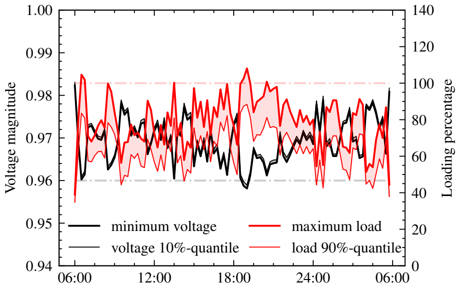

Fig. 9. Grid states at peak shaving at day 1.

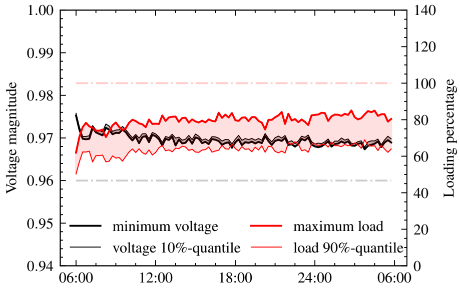

Fig. 10. Grid states at power flow control at day 1.

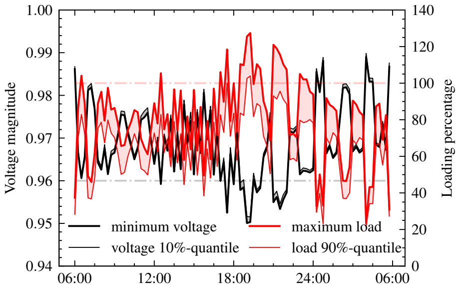

Fig. 11. Grid states at base case at day 2.

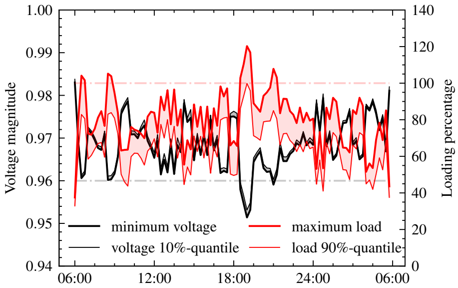

Fig. 12. Grid states at peak shaving at day 2.

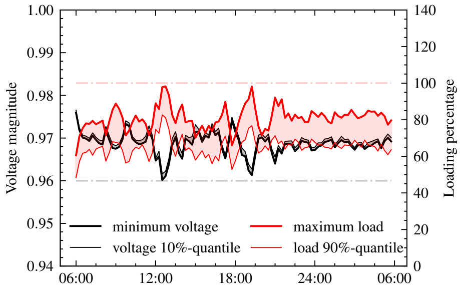

Fig. 13. Grid states at power flow control at day 2.

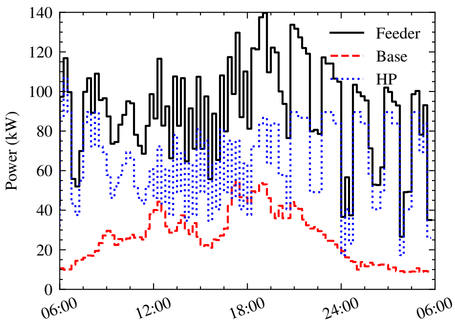

Fig. 14. Feeder load at base case at day 2.

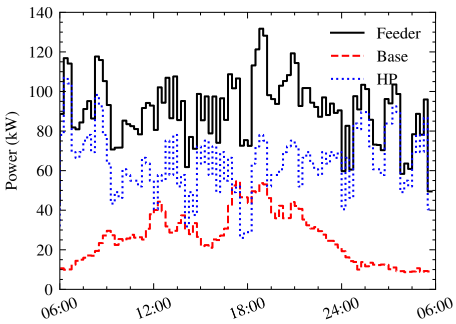

Fig. 15. Feeder load at peak shaving at day 2.

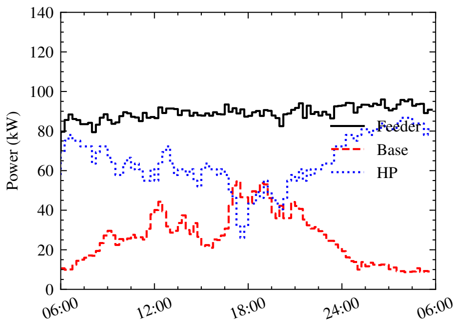

Fig. 16. Feeder load at power flow control at day 2.

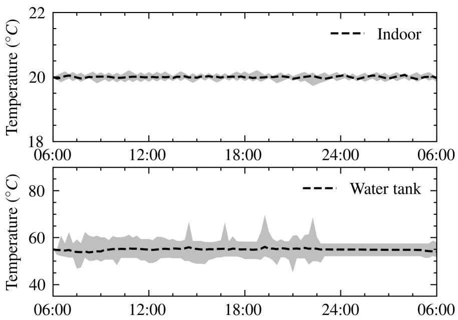

Fig. 17. Thermal comfort at base case.

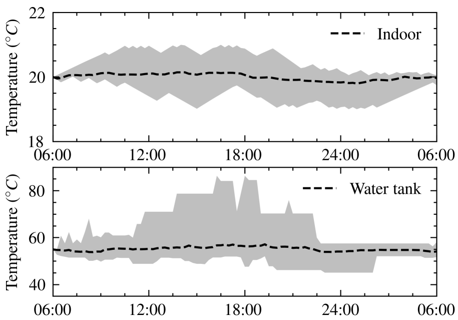

Fig. 18. Thermal comfort with peak shaving.

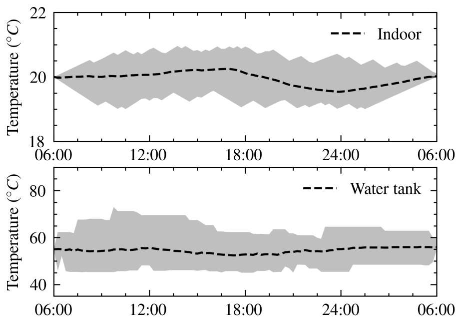

Fig. 19. Thermal comfort with power flow control.

the hosting capacity will be 100% for the peak shaving strategy when the heat transfer coefficient is improved from the current 0.225 kW/K to 0.1 kW/K. Under an even better insulation level with a heat transfer coefficient of 0.05 kW/K, all heat pumps can be safely connected without control due to significantly reduced thermal loss and thus needed energy.

V. Conclusions

In this paper, we investigate the heat pump hosting capacity in an urban housing area with an existing LV feeder. Approximately 70% of the houses are being renovated by the social housing company by replacing gas heating with electric heat pumps. We determine that the hosting capacity for the test LV feeder is increased from 49% for the unmanaged case to 51% for the peak shaving and to 100% for the central optimal power flow control with a working forecast algorithm. Based on the simulation results, we provide the following recommendations to improve the hosting capacity. The first strategy is to improve the insulation level of the households. We see that by improving insulation, the feeder can host all heat pump connections using the individual peak shaving strategy. By even better insulating the households, the feeder can handle unmanaged heat pump use due to significantly reduced energy demand. The second recommendation is to use the individual peak shaving strategy. It is determined that this strategy can host 51% heat pump connections with a working forecast and 76% when combined with an accurate baseload forecast. This highlights the importance of

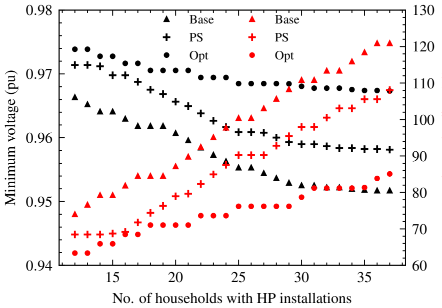

Fig. 20. Hosting capacity with accurate forecast.

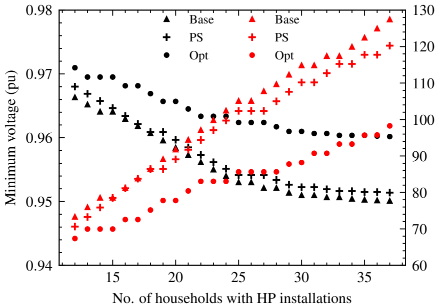

Fig. 21. Hosting capacity with working forecast.

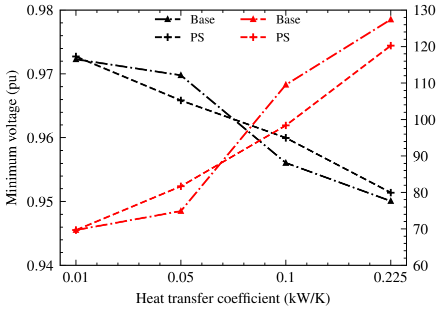

Fig. 22. Impacts of insulation levels.

an accurate baseload forecast algorithm for the individual peak shaving strategy. An alternative to deploying more advanced forecast algorithms is to allow the use of real-time smart meter measurements. If the peak shaving is insufficient, the last recommendation is to use the central optimal power flow control. Although the DSO has to take a more intrusive role in managing heat pumps for end-users, it does not affect the thermal comfort and freedom in demand for end-users. The strategy in the meantime resolves network congestion enabling a higher speed in the transition from gas heating to sustainable heating. This also avoids the risk of severe consequences such as blackouts and drastic loss of thermal comfort for end-users with large-scale unmanaged heat pump connections and use.

References

[1] M. Farrokhseresht, N. G. Paterakis, H. Slootweg *et al.*, "Enabling market participation of distributed energy resources through a coupled market design," *IET Renew. Power Gener.*, vol. 14, no. 4, 2020.

[2] S. C. Doumen, P. Nguyen, and K. Kok, "The State of the Art in Local Energy Markets: A Comparative Review," *IEEE PowerTech*, 2021.

[3] X. Jin, Q. Wu, and H. Jia, "Local flexibility markets: Literature review on concepts, models and clearing methods," *Appl. Energy*, 2020.

[4] R. Li, Q. Wu, and S. S. Oren, "Distribution locational marginal pricing for optimal electric vehicle charging management," *IEEE Trans. Smart Grid*, vol. 9, no. 2, 2014.

[5] L. Bai, J. Wang, C. Wang *et al.*, "Distribution Locational Marginal Pricing (DLMP) for Congestion Management and Voltage Support," *IEEE Trans. Power Syst.*, vol. 33, no. 4, 2018.

[6] J. Hu, G. Yang, H. W. Bindner *et al.*, "Application of Network-Constrained Transactive Control to Electric Vehicle Charging for Secure Grid Operation," *IEEE Trans. Sustain. Energy*, vol. 8, no. 2, 2017.

[17] M. E. Baran and F. F. Wu, "Network Reconfiguration in Distribution Systems for Loss Reduction and Load Balancing," *IEEE Trans. Power Deliv.*, vol. 4, no. 2, pp. 1401–1407, 1989.

[7] J. Hu, G. Yang, C. Ziras *et al.*, "Aggregator Operation in the Balancing Market Through Network-Constrained Transactive Energy," *IEEE Trans. Power Syst.*, vol. 34, no. 5, 2019.

[8] C. Ziras, C. Heinrich, and H. W. Bindner, "Why Baselines Are Not Suited for Local Flexibility Markets," *Renew. Sustain. Energy Rev.*, 2021.

[9] N. Nazir and M. Almassalkhi, "Voltage positioning using co-optimization of controllable grid assets in radial networks," *IEEE Trans. Power Syst.*, 2020.

[10] K. Petrou, A. T. Procopiou, L. Gutierrez-Lagos *et al.*, "Ensuring Distribution Network Integrity Using Dynamic Operating Limits for Prosumers," *IEEE Trans. Smart Grid*, 2021.

[11] S. Zhan, J. Morren, W. v. d. Akker *et al.*, "Combined MV-LV Power Grid Operation : Comparing Sequential, Integrated, and Decentralized Control Architectures," in *Int. Conf. Smart Energy Syst. Technol.*, 2022.

[12] V. Rigoni, D. Flynn, and A. Keane, "Coordinating Demand Response Aggregation with LV Network Operational Constraints," *IEEE Trans. Power Syst.*, vol. 36, no. 2, pp. 979–990, 2021.

[13] P. Yu, C. Wan, M. Sun *et al.*, "Distributed Voltage Control of Active Distribution Networks with Global Sensitivity," *IEEE Trans. Power Syst.*, 2022.

[14] Z. Chen, C. Ziras, and H. W. Bindner, "Towards an Assessment Framework for Congestion Management Mechanisms in Distribution Networks," *IEEE PES Innov. Smart Grid Technol. Europe*, 2021.

[15] G. Verhoeven, B. v. d. Holst, and S. C. Doumen, "Modeling a Domestic All-Electric Air-Water Heat-Pump System for Discrete-Time Simulations," in *Int. Univ. Power Eng. Conf. (UPEC)*, 2022.

[16] J. Leprince, H. Madsen, C. Miller *et al.*, "Fifty shades of grey: Automated stochastic model identification of building heat dynamics," *Energy Build.*, 2022.

[18] E. M. S. Duque, P. P. Vergara, P. H. Nguyen *et al.*, "Conditional Multivariate Elliptical Copulas to Model Residential Load Profiles from Smart Meter Data," *IEEE Trans. Smart Grid*, vol. 12, no. 5, 2021.

[19] O. Ruhnau, L. Hirth, and A. Praktiknjo, "Time series of heat demand and heat pump efficiency for energy system modeling," *Sci. Data*, 2019.

[20] U. Jordan and K. Vajen, "DHWcalc: Program to Generate Domestic Hot Water Profiles With Statistical Means for User Defined Conditions," in *ISES Solar World Congress*, 2005.